CEAI, Vol.28, No.2, pp. 3-11, 2026 Printed in Romania

A Finite-time Control Law Synthesis Method for a Class of Nonlinear Systems based on Differential Geometry Approach

Chiem X. Nguyen*, Hai N. Phan, Nikolay B. Filimonov***, Phong Q. Pham******

** Le Quy Don Technical University, No. 236 Hoang Quoc Viet, Hanoi, Vietnam, (chiemnx@mta.edu.vn)*
*** Le Quy Don Technical University, No. 236 Hoang Quoc Viet, Hanoi, Vietnam, (haipn@lqdtu.edu.vn)*
**** Lomonosov Moscow State University, Moscow, Russia, (nbfilimonov@mail.ru)*
***** Bauman Moscow State Technical University, Moscow, Russia, (hvktqs1421996@gmail.com)*
** chiemnx@mta.edu.vn (Corresponding Author)*

Abstract: In this paper, a finite-time control synthesis method is presented for a class of nonlinear systems. The proposed method is based on a differential geometric approach, in which a virtual system that is finite-time stable with a strict-feedback form is constructed and is diffeomorphic to the system under consideration (i.e., the real system). The control law is derived via a transformation from the real system to the virtual system. This control law ensures that the original system has the same dynamic characteristics as the virtual system and is finite-time stable. The stability in finite-time control of the virtual system is analyzed based on the Lyapunov function. Theoretical analyses and numerical simulations are conducted on three systems and compared with existing methods to demonstrate the effectiveness of the proposed control law.

Keywords: Finite-time control; Fixed-time control; Differential geometry; Nonlinear control systems; Lyapunov-based analysis, Backstepping control

1. INTRODUCTION

In modern control theory, for different types of nonlinear systems, various control methods have been developed based on strict-feedback form and output feedback. Various approaches have been proposed, such as feedback inverse linearization, state/output feedback linearization, dynamic inversion, higher-order sliding modes, Lyapunov-based synthesis, adaptive control, sliding mode control, and fuzzy neural network methods, etc. Among them, a large number of studies apply Lyapunov function in finding control laws for nonlinear systems (Barbashin, 1967; Khalil, 2003; Kim, 2004). The study (Barbashin, 1967) has given some results on the settling time to evaluate the control quality of the system. The studies using backstepping methods, sliding mode control based on strict-feedback systems are presented in the study (Zhang et al., 2000). For non-strict feedback systems, an effective tool used is to decompose the system into subsystems proposed in (Yu et al., 2018). For the case of unmeasurable states, observers are used. These observers have been proposed in the works (Xiao et al., 2020; Tong et al., 2011). Fast convergence is one of the key performance indicators in automatic control systems, which characterizes the corresponding convergence speed. Furthermore, to obtain better performance, faster stabilization time has been a focus of research in practice. The works that present a relatively complete relationship between Lyapunov theory and stabilization time and its application to systems are presented in (Bhat et al., 2000; Yu et al., 2018). Based on finite-time and fixed-time control techniques, numerous studies have demonstrated their ability to guarantee system states converge to the equilibrium point within a finite-time, achieving faster convergence and improved robustness compared to traditional asymptotic stabilization methods. Recent studies (Yu et al., 2018; Polyakov, 2012; Tian et al., 2023) have proposed various finite-time control laws that enhance convergence speed and strengthen robustness against model uncertainties. These techniques have been effectively applied to various classes of nonlinear systems such as electromechanical systems, power converters, robotic mechanisms, and systems with state constraints, thereby confirming their superiority in improving control performance and transient response characteristics. However, developing a generalized control law for a broader class of nonlinear models remains challenging due to the inherent complexity in selecting appropriate Lyapunov functions and establishing finite-time stability conditions.

The differential geometry approach to the synthesis of control laws for nonlinear systems allows researchers to consider the fundamental problems of control theory from a much broader perspective, namely the problems of controllability, observability, invariance, decomposability and composability (Jurdjevic, 1997; Pupkov and Yelutin, 2004; Miroshnik, 2006; Agrachev and Sachkov, 2005; Krasnoshchechenko and Krishchenko, 2005). This approach is particularly useful for the study of nonlinear control systems. The main idea of differential geometry is the application of mathematical analysis and geometrical images to the explanation of dynamic processes. In the problem of synthesizing control laws for nonlinear systems, the differential geometry approach provides a general idea of the structure and dynamics of states in multidimensional space. As a result, the quality of transient processes can be evaluated explicitly. Once the control laws are parameterized, they can be designed to adjust the process quality according to specific criteria, such as convergence time. The paper by (Brockett, 2014) discusses the early stages of development in the field of nonlinear control based on differential geometry, including an overview of the broad background of differential geometry-based control theory since the 1970s. The paper (Pan, 2001).) studies the problem of complete linearization by negative feedback for a stochastic nonlinear system with one input – one output. By using the invariant rule under the micromanifold transformation proposed by the author, the coordinate-independent necessary and sufficient conditions for the control signal finding ability are obtained. The study (Kolar et al., 2021) has demonstrated that any time-discrete nonlinear system with planarity can be decomposed through micromanifold transformations into a subsystem with a lower dimension and an endogenous dynamic response. The study (Marino and Kokotovic, 1988) applies two-time-scale singular perturbation methods to nonlinear systems. The main result of this paper is a coordinate-independent description of the time scales through invariant manifolds that represent the conservation and equilibrium properties of the control system. The study (Nguyen et al., 2019) gives a synthesis of control laws through a quasi-time optimal virtual system based on this approach. The study (Nguyen et al., 2025) used the differential geometry method to synthesize finite-time control law for flexible-joint manipulator, simulation and experimental results showed the effectiveness of this method.

Based on the above discussions, this paper proposes a finite-time control law synthesis method for a class of strict-feedback nonlinear SISO systems based on the differential-geometric approach. First, a virtual system with finite-time stability is constructed, whose convergence characteristics can be adjusted through its design parameters. Next, a diffeomorphism between the original nonlinear system and the virtual system is established, and the existence of this transformation is verified. The actual control law is then derived through this diffeomorphic transformation, allowing the desired finite-time behavior of the virtual system to be transferred to the original system. The stability and finite-time convergence properties are analyzed using the Lyapunov method.

The main contribution of this paper is the development of a differential-geometry-based finite-time control synthesis framework that separates the design procedure into two stages: shaping the desired finite-time dynamics in a virtual system and mapping these dynamics back to the original nonlinear system. Compared with conventional backstepping-based finite-time controllers, which usually require recursive Lyapunov-function construction and complicated parameter tuning, the proposed framework provides a more transparent design mechanism. Moreover, the convergence behavior can be adjusted through the virtual-system parameters. Simulation results show that the proposed controllers achieve faster transient response, smaller tracking errors, and reduced oscillatory behavior compared with the traditional backstepping method.

The remainder of this paper is organized as follows. Section 2 presents the preliminaries and the problem formulation, including the class of nonlinear systems considered, stability concepts, and finite-time boundedness. Section 3 develops the finite-time stable virtual system and the proposed control law synthesis method. Section 4 provides three simulation examples to demonstrate the effectiveness of the proposed control laws and compare their performance with the traditional backstepping method. Finally, Section 5 concludes the paper and outlines future research directions.

2. PRELIMINARIES AND PROBLEM FORMULATION

2.1 Mathematical model of the object

Consider the following class of n-order SISO nonlinear systems:

$$\begin{cases} \dot{x}_1 = f_1(\bar{x}_1) + g_1(\bar{x}_1)x_2 \\ \dot{x}_2 = f_2(\bar{x}_2) + g_2(\bar{x}_2)x_3 \\ \vdots \\ \dot{x}_n = f_n(\bar{x}_n) + g_n(\bar{x}_n)u \end{cases} \tag{1}$$

where $x = [x_1, x_2, \ldots, x_n]^T \in R^n$ is the state vector with $x(0) = x_0$, $\bar{x}_i = [x_1, x_2, \ldots, x^i]^T$ and u is the control signal. The functions $f_i(\cdot)$ and $g_i(\cdot)$ (i = 1, 2, .., n) are considered to be known. The symbol x_{1d} denotes the desired reference signal and its derivative is considered to be a smooth, bounded and known function. The control law u needs to be synthesized so that the output x_1 follows the reference signal x_{1d} from any initial condition in finite-time and all states of the closed-loop system are bounded in finite-time. To synthesize the control law for system (1), the following Assumption 1 must be imposed.

Assumption 1 (Yu et al., 2018): There exists an open set $\Omega_d \subset R^n$ consisting of the origin and initial condition x_0. The functions $f_i(\cdot)$ and $g_i(\cdot)$ are bounded in the closed set Ω_d; their derivatives up to order n-i are bounded in the closed set Ω_d; there exist known positive constants η and ρ such that $\eta < |gi| < \rho$.

2.2 Differential geometry in equivalence transformation

Nonlinear transformation of state space is a powerful mathematical tool for studying the motion of dynamical systems. According to (Miroshnik, 2006), for equivalence transformation of autonomous systems, it is necessary to construct a smooth one-to-one mapping and there exists a corresponding smooth inverse mapping. The model of this transformation can be expressed in the following form.

Consider the following autonomous dynamical systems:

$$\dot{x} = f(x), \tag{2}$$

and

$$\dot{z} = \phi(z) \tag{3}$$

where $x \in X \subset R^n$, $z \in Z \subset R^n$, f and ϕ are smooth vector functions defined on some sets X and Z, respectively. The transformation of the state space between (2) and (3) is carried out by the mapping:

$$z = \varphi(x). \tag{4}$$

The equivalence condition of these two systems is determined by the diffeomorphism φ: $X \to Z$, which has a non-degenerate Jacobian matrix [10], i.e:

$$det\left[\frac{\partial z}{\partial x}\right] \neq 0. \tag{5}$$

The special feature of this transformation is the preservation of the topological properties of the state space, which enables a meaningful comparison of dynamical behaviors between systems. Furthermore, the theorem on the equivalence of asymptotic stability properties of two systems (2) and (3) is presented in the study by (Miroshnik, 2006; Agrachev and Sachkov, 2005). Additionally, the concept of state space transformation is often employed in automatic control systems to investigate the properties of observability and controllability (Krasnoshchechenko and Krishchenko, 2005).

2.3 Finite-time control fundamentals

Finite-time stability is defined by the requirement that every trajectory reaches the origin within a finite duration, which represents a stricter condition compared to asymptotic stability. Classical results, such as those in (Bhat and Bernstein, 2000; Polyakov, 2012), provide sufficient criteria for ensuring that the origin of system (2) is a stable equilibrium in finite time. This property guarantees convergence to the origin within a time that depends on the initial state, whereas fixed-time stability ensures convergence within a uniformly bounded interval that is independent of initial conditions (Polyakov, 2012). Throughout this paper, ‖·‖ denotes the Euclidean norm.

Definition 1 (Amato et al., 2014): The solution of nonlinear system (2) is said to be finite-time ultimately bounded with a prescribed ultimate bound Δ if, for a prescribed constant $\Delta > 0$ and for every initial condition $x(t_0) = x_0$, there exists a finite settling time $T(\Delta, x_0) < \infty$ such that $\|x(t)\| < \Delta$ for all $t > t_0 + T$. This means that the state trajectory enters and remains inside the prescribed neighborhood of the origin with radius Δ after a finite time.

Lemma 1 (Yu et al., 2018): Consider the nonlinear system (2), suppose that there is a Lyapunov function $V(x)$, $c>0$, $k>0$, and $0<\alpha<1$ such that

$$\dot{V}(x) + cV^{\alpha}(x) + kV(x) \le 0, \quad \forall x \in U \tag{6}$$

holds. Then, the equilibrium $x = 0$ is finite-time stable, and the convergence time of the system (2) is given by:

$$T(x_0) \le \frac{ln(1 + (k/c)V^{1-\alpha}(x_0))}{k(1-\alpha)} \tag{7}$$

Lemma 2 (Polyakov, 2012): Consider the nonlinear system (2), assume that there is a C^1 function $V(x)$: $R^n \to R^+ \cup \{0\}$ satisfying

$$\dot{V}(x) \le -[\gamma_1 V^p(x) + \gamma_2 V^q(x)]^k \tag{8}$$

where $\gamma_1>0$, $\gamma_2>0$, $p>0$, $q>0$, $k>0$, $pk<1$, and $qk>1$. Then, the equilibrium $x=0$ is fixed-time stable, and the settling time of system (2) is estimated by

$$T(x_0) \le T_{max} = \frac{1}{\gamma_1^k(1-pk)} + \frac{1}{\gamma_2^k(qk-1)} \tag{9}$$

3. SYNTHESIS OF FINITE-TIME CONTROL LAWS FOR SISO NONLINEAR SYSTEMS

3.1 Systems with finite-time characteristics

This section introduces virtual systems designed to exhibit finite-time convergence characteristics to synthesize control laws. The virtual system with fixed finite-time characteristics is built based on the strict-feedback system of the form:

$$\begin{cases} \dot{z}_i = -v_i z_i + z_{i+1}; & i = \overline{1, n-1},\ v_i > 0; \\ \dot{z}_n = \tau \end{cases}, \tag{10}$$

where $z_i, i = \overline{1,n}$ are the states of the system, τ is the control signal.

Lemma 3. Consider system (10) with control law (11) :

$$\tau = \left(-\frac{c}{2^{\alpha}} sgn(s)|s|^{2\alpha-1} - \frac{k}{2}s + \sum_{i=1}^{n-1}(v_i c_i z_i - c_i z_{i+1}) \right) / c_n \tag{11}$$

and $A \in R^{n-1\times n-1}$ is a Hurwitz matrix and satisfies the following Lyapunov equation:

$$A^T P + PA = -I \tag{12}$$

where: P is positive definite symmetric matrix and $s = \sum_{i=1}^{n} c_i z_i$; $c > 0$; $k > 0$; $\alpha \in (0.5,1)$; $c_i > 0, i = \overline{1,n}$.

If the matrix A is of the following form:

$$A = \begin{bmatrix} -v_1 & 1 & \cdots & 0 \\ 0 & -v_2 & 1 & \cdots \\ 0 & \cdots & \ddots & 1 \\ -\frac{c_1}{c_n} & \cdots & -\frac{c_{n-2}}{c_n} & -v_{n-1} - \frac{c_{n-1}}{c_n} \end{bmatrix}, \tag{13}$$

then system (10) converges to the neighborhood of the origin with radius Δ in finite time for any initial condition z_0.

Proof:

Consider Lyapunov function:

$$V = \frac{1}{2}s^2 \tag{14}$$

By taking the time derivative, the following expression is obtained:

$$\dot{V} = s\dot{s} = s\left(\sum_{i=1}^{n-1}(-v_i c_i z_i + c_i z_{i+1}) + c_n \tau \right) \tag{15}$$

Substituting τ into (15) and using $V \ge 0$ from (14) gives:

$$\begin{aligned} \dot{V} &= s\left(\sum_{i=1}^{n}(-v_i c_i z_i + c_i z_{i+1}) - \frac{c}{2^{\alpha}} sgn(s)|s|^{2\alpha-1} - \frac{k}{2}s + \sum_{i=1}^{n-1}(v_i c_i z_i - c_i z_{i+1}) \right) = \\ &= s\left(-\frac{c}{2^{\alpha}} sgn(s)|s|^{2\alpha-1} - \frac{k}{2}s \right) \\ &= -\frac{c}{2^{\alpha}}(s^2)^{\alpha} - \frac{k}{2}s^2 \\ &= -cV^{\alpha} - kV \le 0 \end{aligned} \tag{16}$$

From this, it is clear that the proposed control law ensures that system (10) evolves on the manifold $s=0$, with the settling time T calculated according to formula (7). The next step is to prove that the evolution of the system on the manifold $s=0$ leads system (10) to converge to the neighborhood Δ of the origin.

For $s=0$, it follows that:

$$z_n = -\frac{1}{c_n}\sum_{i=1}^{n-1} c_i z_i \quad (17)$$

Substitute (17) into equation (10) and write it in the following form:

$$\dot{\bar{z}} = A\bar{z} \quad (18)$$

where $\bar{z} = [z_1, z_2, \ldots, z_{n-1}]^T$ is the vector ($\bar{z} \in R^{n-1}$), A is a square matrix of the form (13). For the reduced system described by (18), the initial condition is taken at the time when the trajectory reaches the manifold $s=0$. Let T denote this finite reaching time, as estimated by (7), and let $\bar{z}(T) = \bar{z}_0$. By resetting the time origin at T, the settling time of the reduced system is analyzed as follows. Let t_p denote the first time instant, measured from T, at which the trajectory $\bar{z}(t)$ enters and thereafter remains inside the Δ-neighborhood of the origin. Equivalently, $t_p = \inf\{t \geq 0 \colon \|\bar{z}(\xi)\| \leq \Delta, \forall \xi \geq t\}$.

To establish the convergence of the reduced system, consider the following Lyapunov function:

$$V(\bar{z}) = \bar{z}^T P \bar{z} \quad (19)$$

By taking the time derivative of V and applying condition (12), the following is obtained:

$$\dot{V}(\bar{z}) = -\bar{z}^T\bar{z} = -\|\bar{z}\|^2 \quad (20)$$

Using the properties of the quadratic form:

$$\lambda_m\|\bar{z}\|^2 \leq V(\bar{z}) \leq \lambda_M\|\bar{z}\|^2 \quad (21)$$

$$-\frac{V(\bar{z})}{\lambda_m} \leq -\|\bar{z}\|^2 \leq -\frac{V(\bar{z})}{\lambda_M}, \quad (22)$$

with λ_m being the smallest eigenvalue and λ_M the largest eigenvalue of the matrix P.

From (20) and (21), the following inequality is obtained:

$$-\frac{dt}{\lambda_m} \leq \frac{dV(\bar{z})}{V(\bar{z})} \leq -\frac{dt}{\lambda_M} \quad (23)$$

By integrating this inequality, the following is obtained:

$$V_0 e^{-\frac{t}{\lambda_m}} \leq V(\bar{z}) \leq V_0 e^{-\frac{t}{\lambda_M}} \quad (24)$$

where:

$$V_0 = \bar{z}_0^T P \bar{z}_0. \quad (25)$$

From inequality (24), combined with inequality (22), the following is obtained:

$$V_0 e^{\frac{-t}{\lambda_M}} \geq \lambda_m\|\bar{z}\|^2 \quad (26)$$

If t_p denotes the response time of the system to move from the initial position to the desired region ($\|\bar{z}\|^2 \leq \Delta^2$), the following is obtained:

$$t_p \leq \lambda_M \, ln\frac{V_0}{\lambda_m \Delta^2} \quad (27)$$

The above analysis shows that the trajectory reaches the manifold $s=0$ within the finite reaching time T estimated by (7). After reaching this manifold, the reduced system (18) drives $\bar{z}$ into the prescribed Δ-neighborhood of the origin within the finite time t_p estimated by (27). Hence, the total convergence time can be estimated as $T_{FT} \leq T + t_p$. Therefore, according to Definition 1, system (10) is finite-time ultimately bounded with the prescribed ultimate bound. In addition, the convergence time of system (10) under the control law (11) can be adjusted by tuning both the reaching time to the manifold $s=0$ and the convergence time of the reduced system (18) to the region Δ.

Lemma 4. Consider the system (10) with the control law (28)

$$\tau = \left(-sgn(s)\left(\frac{\gamma_1}{2^p}|s|^{2p-\frac{1}{k}} + \frac{\gamma_2}{2^q}|s|^{2q-\frac{1}{k}}\right)^k + \sum_{i=1}^{n-1}(v_i c_i z_i - c_i z_{i+1})\right)/c_n \quad (28)$$

and $A \in R^{n-1 \times n-1}$ is a Hurwitz matrix and satisfies the following Lyapunov equation:

$$A^T P + PA = -I \quad (29)$$

where P is a positive definite symmetric matrix, and $s = \sum_{i=1}^{n} c_i z_i$; $k > 0; p > \frac{1}{2k}; q > \frac{1}{2k}$; $\gamma_1 > 0; \gamma_2 > 0; c_i > 0, i = \overline{1,n}.$

If the matrix A is as in formula (13), then system (10) converges to the neighborhood of the origin with radius Δ in finite time for any initial condition z_0.

Proof: Following an argument similar to the proof of Lemma 3, the virtual system (10) reaches the manifold $s=0$ within a fixed finite time estimated by (9). Subsequently, the reduced system (18) drives $\bar{z}$, and consequently the state z, into the prescribed Δ-neighborhood of the origin within the finite time estimated by (27).

3.2 Synthesis of finite-time control laws for nonlinear SISO systems

The main idea of applying differential geometry theory in this work is to find the differential transformation between the original system and some virtual systems. Consequently, this transformation is undertaken by the control law that will be synthesized and have finite-time characteristics. Pointing out the differential transformation will ensure that the synthesized control law is able to stabilize the system in fixed finite-time. The original system is described by the mathematical model (1) and serves as the basis for designing the virtual system (10). This virtual system maintains similar dynamics while offering qualitative improvements, such as finite and fixed convergence times.

Theorem 1. Consider the system (1) with Assumption 1 and the virtual system (10) satisfying Lemma (3). If the diffeomorphism is constructed as in the following system (30):

$$\begin{cases} z_1 = \varphi_1(\bar{x}_1) = x_1 - x_{1d}; \\ z_2 = \varphi_2(\bar{x}_2) = \dot{z}_1 + v_1 z_1 \\ \quad = f_1(\bar{x}_1) + g_1(\bar{x}_1)x_2 \\ \quad -\dot{x}_{1d} + v_1(x_1 - x_{1d}); \\ \vdots \\ z_n = \varphi_n(\bar{x}_n) = \dot{z}_{n-1} + v_{n-1}z_{n-1} = \\ = \sum_{i=1}^{n-1} \frac{\partial \varphi_{n-1}}{\partial x_i}\left(f_i(\bar{x}_i) + g_i(\bar{x}_i)x_{i+1}\right) - \\ \quad x_{1d}^{(n-1)} + v_{n-1}\varphi_{n-1}(\bar{x}_{n-1}) \end{cases}, \tag{30}$$

and the control signal is constructed as in (31), then the system of equations (1) converges to a region around the origin with radius Δ in a finite-time interval (27).

$$u = \left(\frac{\partial \varphi_{n-1}}{\partial x_{n-1}} g_{n-1}(\bar{x}_{n-1}) g_n(\bar{x}_n)\right)^{-1} \times \left(\begin{array}{l} \tau - \sum_{j=1}^{n-1} \frac{d}{dt}\left(\frac{\partial \varphi_{n-1}}{\partial x_j}\right)\left(f_j(x_j) + g_j(x_j)x_{j+1}\right) \\ -\sum_{j=1}^{n-2} \frac{\partial \varphi_{n-1}}{\partial x_j} \frac{d}{dt}\left(f_j(\bar{x}_j) + g_j(\bar{x}_j)x_{j+1}\right) \\ -\frac{\partial \varphi_{n-1}}{\partial x_{n-1}}\left(\begin{array}{l} \sum_{i=1}^{n-1} \frac{\partial f_{n-1}}{\partial x_i}\dot{x}_i + x_n \sum_{i=1}^{n-1} \frac{\partial g_{n-1}}{\partial x_i}\dot{x}_i \\ +g_{n-1}(\bar{x}_{n-1}) f_n(\bar{x}_n) \end{array} \right) \\ +x_{1d}^{(n)} - v_{n-1}\sum_{i=1}^{n-1} \frac{\partial \varphi_{n-1}}{\partial x_i}\dot{x}_i \end{array} \right) \tag{31}$$

Proof: Based on condition (5) and the transformation from the original system (1) to the virtual system (10) as in (30), the determinant of the Jacobian matrix is obtained:

$$det \begin{bmatrix} \frac{\partial \varphi_1}{\partial x_1} & 0 & \cdots & 0 \\ \frac{\partial \varphi_2}{\partial x_1} & \frac{\partial \varphi_2}{\partial x_2} & \cdots & 0 \\ \vdots & \vdots & \cdots & \vdots \\ \frac{\partial \varphi_n}{\partial x_1} & \frac{\partial \varphi_n}{\partial x_2} & \cdots & \frac{\partial \varphi_n}{\partial x_n} \end{bmatrix} = \prod_{i=1}^{n} \frac{\partial \varphi_i}{\partial x_i} = \prod_{i=1}^{n-1} g_i(\bar{x}_i) \neq 0 \tag{32}$$

By assumption 1, condition (5) is always true. Therefore, transformation (30) always exists. Then the control law is found recursively from the last equation of system (10) and from the diffeomorphism (30) for system of equations (1) as follows:

$$\dot{z}_n = \tau$$
$$\frac{d\left(\begin{array}{c} \sum_{i=1}^{n-1} \frac{\partial \varphi_{n-1}}{\partial x_i}\left(f_i(\bar{x}_i) + g_i(\bar{x}_i)x_{i+1}\right) \\ -x_{1d}^{(n-1)} + v_{n-1}\varphi_{n-1}(\bar{x}_{n-1}) \end{array} \right)}{dt} = \tau \tag{33}$$

Combined with the system of equations (1), the following is obtained:

$$u = \left(\frac{\partial \varphi_{n-1}}{\partial x_{n-1}} g_{n-1}(\bar{x}_{n-1}) g_n(\bar{x}_n)\right)^{-1} \times \left(\begin{array}{l} \tau - \sum_{j=1}^{n-1} \frac{d}{dt}\left(\frac{\partial \varphi_{n-1}}{\partial x_j}\right)\left(f_j(x_j) + g_j(x_j)x_{j+1}\right) \\ -\sum_{j=1}^{n-2} \frac{\partial \varphi_{n-1}}{\partial x_j} \frac{d}{dt}\left(f_j(\bar{x}_j) + g_j(\bar{x}_j)x_{j+1}\right) \\ -\frac{\partial \varphi_{n-1}}{\partial x_{n-1}}\left(\begin{array}{l} \sum_{i=1}^{n-1} \frac{\partial f_{n-1}}{\partial x_i}\dot{x}_i + x_n \sum_{i=1}^{n-1} \frac{\partial g_{n-1}}{\partial x_i}\dot{x}_i \\ +g_{n-1}(\bar{x}_{n-1}) f_n(\bar{x}_n) \end{array} \right) \\ +x_{1d}^{(n)} - v_{n-1}\sum_{i=1}^{n-1} \frac{\partial \varphi_{n-1}}{\partial x_i}\dot{x}_i \end{array} \right) \tag{34}$$

It should be noted that if the control law determined from (34), when substituted into (1) ensures the condition (32), then it ensures the stability of the entire system. Furthermore, it can be proved that the system (1) with the control law (34) ensures the system is stable with the finite-time of the virtual system (10) according to the similarity of differential geometry.

Theorem 2. Consider the system (1) with Assumption 1 and the virtual system (10) satisfying Lemma (4). If the differential transformation is constructed as in the system (30), the control signal is constructed as in the form (31), then the system of equations (1) converges to a region around the origin with radius *Δ* in the finite-time interval (27).

Proof: Similar to Theorem 1.

Remark 1: In the components of τ in formulas (11) and (28) contains the sign function component *sign(s)*. But this component multiplies expressions that depend on s and will go to *0* as *s* goes to *0*. Therefore, the control law does not induce chattering as the system approaches the sliding surface, which is commonly observed in conventional sliding-mode control.

Remark 2: The parameters of τ in formulas (11) and (28) are divided into two groups. The first group, including $c, k, \alpha, p, q, \gamma_1$, and γ_2, is chosen to satisfy the imposed conditions and to ensure the desired convergence time to the manifold *s=0*. The second group $v_i, i = \overline{1, n-1}; c_i, i = \overline{1, n}$, is selected to guarantee convergence to the prescribed neighborhood of the origin within the estimated finite time.

4. NUMERICAL SIMULATIONS AND DISCUSSION

This section presents simulation results for three nonlinear systems to demonstrate the effectiveness of the proposed control synthesis method. The performance is compared with the backstepping method to highlight improvements in tracking accuracy and convergence time.

Example 1:

This example presents a comparison between the technique of this paper and the backstepping method proposed in (Khalil, 2003). The control object here is the electromechanical system whose diagram is shown in Figure 1 (Tong et al., 2011; Yu et al., 2018).

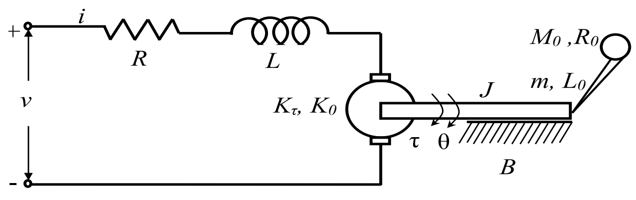

Fig. 1. Electromechanical system diagram.

The dynamics of an electromechanical system is described by the following equation (Tong et al., 2011):

$$\begin{aligned} &M\ddot{\theta} + B\dot{\theta} + N\sin(\theta) = I \\ &L\dot{I} + RI = V - K_B\dot{\theta} \end{aligned} \qquad (35)$$

where $M = \frac{1}{K_\tau}\left(J + \frac{mL_0^2}{3} + M_0L_0^2 + \frac{2M_0R_0^2}{5}\right)$, $N = \frac{L_0G}{K_\tau}\left(\frac{m}{3} + M_0\right)$, J is the rotor inertia, M is the linkage mass, M_0 is the load mass, L_0 is the linkage length, R_0 is the load radius, G is the gravity coefficient, B_0 is the viscous friction coefficient at the joint, θ is the angular position of the motor (and therefore the load), I is the motor armature current, and K_τ is the coefficient characterizing the electromechanical conversion of the armature current into torque. L is the armature inductance, R is the armature resistance, K_B is the reverse emf coefficient, and V is the input control voltage. The values of the selected parameters are $J = 1.625\ 10^{-3}\ Kgm^2$, $m = 0.506\ Kg$, $R_0 = 0.023\ m$, $M_0 = 0.434\ Kg$, $L_0 = 0.305\ m$, $B_0 = 16.25\ 10^{-3}\ Nms/rad$, $L = 15\ H$, $R = 5.0\ \Omega$, $K_\tau = 0.90\ Nm/A$, $K_B = 0.90\ Nm/A$.

Let the variables $x_1 = \theta$; $x_2 = \dot{\theta}$, $x_3 = I$ and $u = V$, and the dynamics given by (35) can be rewritten as:

$$\begin{aligned} \dot{x}_1 &= x_2 \\ \dot{x}_2 &= -\frac{B}{M}x_2 - \frac{N}{M}\sin(x_1) + \frac{1}{M}x_3 \\ \dot{x}_3 &= -\frac{K_B}{L}x_2 - \frac{R}{L}x_3 + \frac{1}{L}u \end{aligned} \qquad (36)$$

First, the finite-time control law parameters according to Lemma (3) are selected as follows: $\alpha=0.99$, $c=100$, $v_1=20$, $v_2=20$, $c_1=1$, $c_2=1$, $c_3=1$, $k=1$. The finite-time control law parameters according to Lemma (4) are selected as follows: $p=0.99$, $q=1.2$, $v_1=20$, $v_2=20$, $c_1=1$, $c_2=1$, $c_3=1$, $k=1$, $\gamma_1=100$, $\gamma_2=100$. The simulation is performed with the initial condition chosen to be zero, and the reference signal is $x_d = 0.5\sin(t) + 0.5\sin(0.5t)$. Next, the backstepping method in [2] is also used to control the system (36), with the corresponding controller parameters being $c_1=60$, $c_2=20$, $c_3=40$ and the remaining parameters are chosen the same as the method proposed in this paper. The control signal is limited in the range $[-150,150]$.

The simulation results for the electromechanical, compared with the backstepping control law, are shown in Fig. 2–4. The tracking performance is shown in Fig. 2, from which it can be seen that the tracking performance is still guaranteed and the tracking error is small. For the backstepping method ($x_{1Back.}$), there is still oscillation at the initial time, while the proposed control law ensures that $x_{1Pro.1}$ and $x_{1Pro.2}$ of the motor are stable at the set value without oscillation. It should be noted that this method ensures the system is stable, that is, independent of the initial conditions. Fig. 3 presents the tracking performance, from which it can be seen that the tracking error of the backstepping control law is larger and oscillates, while the proposed control law ensures that the error is close to 0 after a finite period of time. Fig. 4 shows the control law values of the three methods, from which it is clear that the proposed control law only changes slightly in the initial time, while the backstepping control law fluctuates strongly in the initial time. This behavior is undesirable for practical engineering systems. From this result, it can be seen that the proposed finite-time control method provides better tracking performance than the traditional backstepping method.

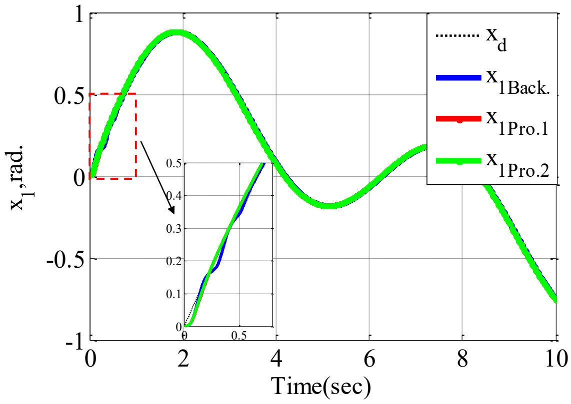

Fig. 2. Tracking performance comparison between the proposed and the backstepping method.

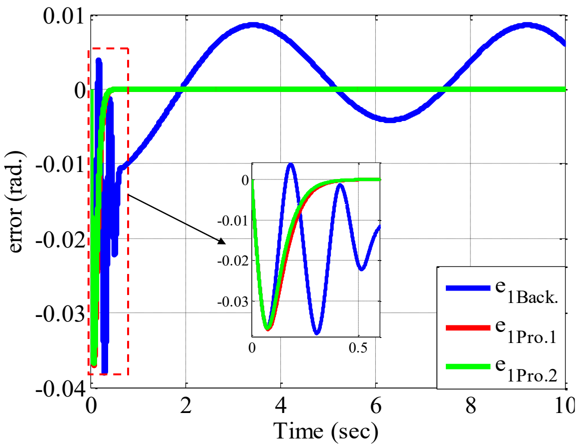

Fig. 3. Control error by the proposed and the backstepping methods.

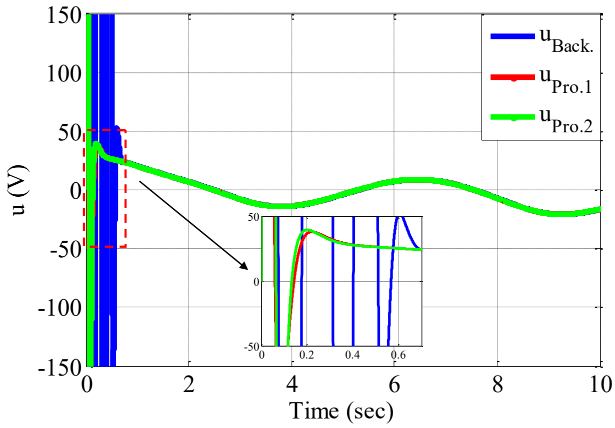

Fig. 4. Control signals by the proposed and the backstepping methods.

Example 2:

In this example, the proposed control laws are synthesized for a flexible joint system. The dynamic model of the flexible joint, presented in the study by (Nguyen et al., 2025), is given as follows:

$$\begin{aligned} \dot{x}_1 &= x_2 \\ \dot{x}_2 &= -\frac{1}{I}(Mgsin(x_1) + K(x_1 - x_3)) \\ \dot{x}_3 &= x_4 \\ \dot{x}_4 &= \frac{1}{J}(K(x_1 - x_3) + u) \end{aligned} \tag{37}$$

In this system, u denotes the control input applied to the soft joint actuator. The model parameters are defined as follows: $M=1$ *(kg)* is the mass of the link; $K=50$ *(Nm/rad)* represents the stiffness of the joint modeled by a linear torsional spring; $I=1(kg\ m^2)$ and $J=1(kg\ m^2)$ denote the link inertia and motor inertia, respectively; $l=1$ *(m)* is the distance to the center of mass of the link; and g =9.8 (m/s^2).

The initial conditions of the system are set at the origin, and the desired reference trajectory for the link angle is given by $x_d=cos(t)$. The parameters of the finite-time control law according to Lemma (3) are selected as: $\alpha=0.99$, $c=100$, $v_1=20$, $v_2=20$, $v_3=20$, $c_1=1$, $c_2=1$, $c_3=1$, $c_4=1$, $k=1$. The parameters of the finite-time control law according to Lemma (4) are chosen as: $p=0.99$, $q=1.2$, $v_1=20$, $v_2=20$, $v_3=20$, $c_1=1$, $c_2=1$, $c_3=1$, $c_4=1$, $k=1$, $\gamma_1=100$, $\gamma_2=100$. The parameters of the Backstepping controller are selected as: $c_1=5$, $c_2=1$, $c_3=5$, $c_4=20$.

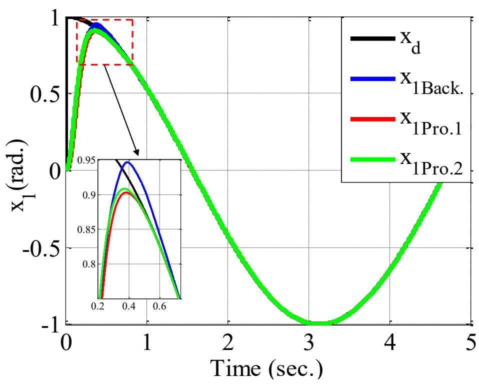

Fig. 5. Response of the link's rotational angle in tracking the desired trajectory x_d.

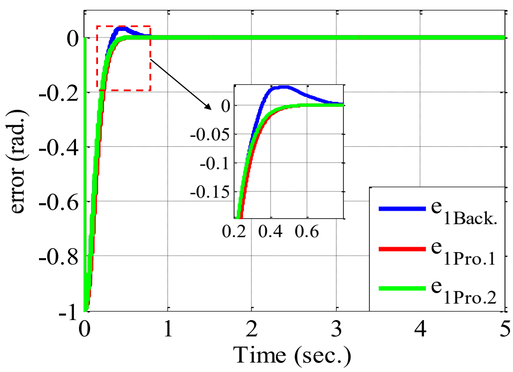

Fig. 6. Tracking error of the link corresponding to the control signals.

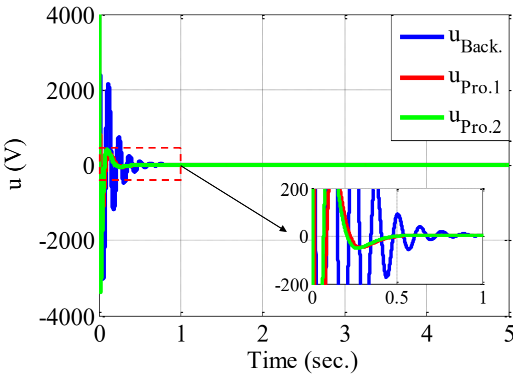

Fig. 7. Control signals generated by the proposed control laws for the flexible-joint manipulator.

The simulation results of Example 2, presented in Figs. 5–7, clearly demonstrate the superior performance of the proposed control laws for the trajectory-tracking problem of the flexible-joint system. Specifically, the link-angle response (Fig. 5) indicates that the two proposed methods ($x_{1Pro.1}$ and $x_{1Pro.2}$) track the desired trajectory rapidly without overshoot and almost coincide with the reference signal. In contrast, the conventional backstepping controller ($x_{1Back.}$) exhibits oscillations and noticeable deviations during the transient phase. The tracking-error analysis (Fig. 6) further shows that the errors corresponding to the proposed methods decrease more rapidly and remain smaller throughout the entire process; in particular, the Pro.2 algorithm achieves near-zero error within a short period of time. Both proposed algorithms suppress the error more effectively, with smaller error magnitudes even from *0.5 s* onward (as highlighted in the zoomed-in region). Moreover, the corresponding control inputs (Fig. 7) also reveal clear advantages, as the proposed methods generate control signals with smaller amplitudes, reduced oscillations, and significantly improved stability compared to the traditional backstepping controller, which produces large and highly oscillatory inputs during the initial phase. These results confirm that the proposed control laws not only enhance trajectory-tracking performance but also offer higher practical feasibility by reducing actuator effort.

Example 3:

Consider the fifth-order nonlinear systems presented in (Yu et al., 2018) of the following form:

$$\begin{aligned} \dot{x}_1 &= x_2 \\ \dot{x}_2 &= -35.55\,sin(x_1) - 0.282x_2 + x_3 \\ \dot{x}_3 &= -0.93x_1x_2 - 5.19x_2 + x_4 \\ \dot{x}_4 &= x_5 \\ \dot{x}_5 &= -sin(x_3) - x_5 + u \end{aligned} \tag{38}$$

The initial conditions and reference signals are chosen the same as in [5]. The finite-time control law parameters according to Lemma (3) are chosen as follows: $\alpha=0.99$, $c=100$, $v_1=20$, $v_2=20$, $v_3=20$, $v_4=20$, $c_1=1$, $c_2=1$, $c_3=1$, $c_4=1$, $c_5=1$, $k=1$. The finite-time control law parameters according to Lemma (4) are chosen as follows: $p=0.99$, $q=1.2$, $v_1=20$; $v_2=20$, $v_3=20$, $v_4=20$, $c_1=1$, $c_2=1$, $c_3=1$, $c_4=1$, $c_5=1$, $k=1$, $\gamma_1=100$, $\gamma_2=100$. Similarly, the backstepping method is evaluated using different parameter sets: $c_1=90$, $c_2=100$, $c_3=100$, $c_4=100$, $c_5=10$.

The simulation results for the object with equation (38) are presented in Fig. 8 to 10. The simulated controllers all ensure that the system tracks the given signal. For high-order objects, the tracking performance with the control law is still guaranteed as shown in Fig. 8, the backstepping controller gives worse tracking quality. The tracking error shows that the proposed controllers quickly converge to 0 in a finite-time but there are still errors, especially at the peak points of the tracking signal. However, the tracking error results are much better than the backstepping method (Fig. 9). In Fig. 10, the control law values of the 3 methods are shown, the control signals do not exhibit excessive peaking or oscillations and do not fluctuate greatly. However, choosing the controller parameters for the backstepping method for high-order systems will be difficult. But with the proposed method it can be clearly seen that the choice of controller parameters can evaluate the stabilization time through the system (10).

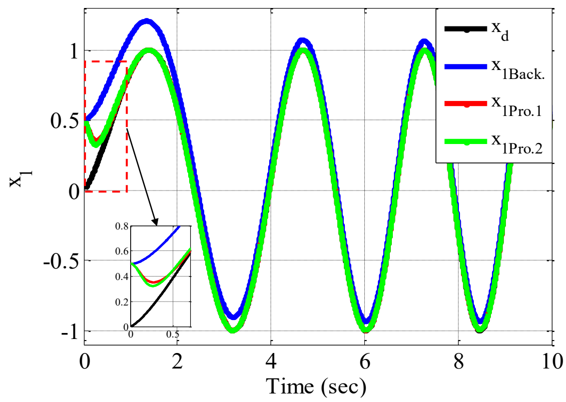

Fig. 8. Control objectives by the proposed and the backstepping methods.

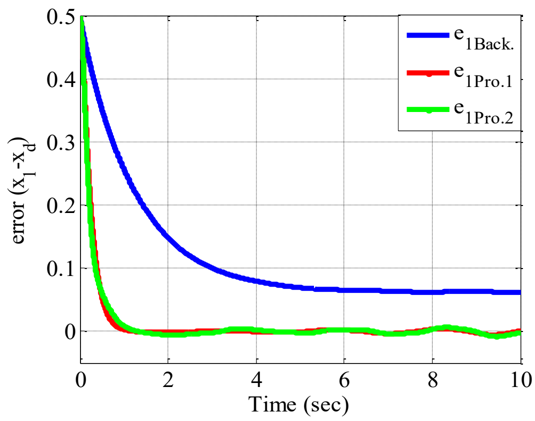

Fig. 9. Control error by the proposed and the backstepping method.

Based on the three simulation examples, the quantitative performance indices for the state x_1 are summarized in Table 1. The proposed controllers achieve smaller tracking errors and shorter transient times than the backstepping controller. Moreover, the control signals generated by the proposed methods exhibit less oscillatory behavior, which is advantageous for practical implementation.

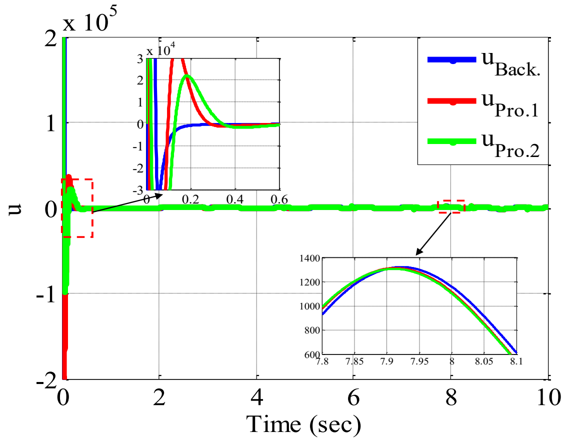

Fig. 10. Control signals by the proposed and the backstepping method.

Table 1. Control Performance Indices.

Example	Controller	Settling time (s)	Steady-state error
1	Back.	1.41	$(-5.0\div9.0)\times10^{-3}$ (rad.)
	Pro.1	0.26	0 (rad.)
	Pro.2	0.24	0 (rad.)
2	Back.	0.32	0 (rad.)
	Pro.1	0.32	0 (rad.)
	Pro.2	0.32	0 (rad.)
3	Back.	∞	0.06
	Pro.1	0.38	$(-8.5\div6.5)\times10^{-3}$
	Pro.2	0.35	$(-5.2\div5.8)\times10^{-3}$

5. CONCLUSIONS

In this paper, a finite-time control law synthesis method for a class of high-order nonlinear systems is proposed based on the differential geometry method. A finite-time stable virtual system is constructed, whose convergence property can be adjusted through its design parameters. A diffeomorphism between the original system and the virtual system is established, and the existence of this transformation is confirmed. Through this diffeomorphic transformation, the proposed control law preserves the finite-time stability properties between the virtual system and the original system. The stability and finite-time convergence properties of the virtual system are proven using the Lyapunov method. These results highlight the role of the proposed differential-geometric transformation in simplifying finite-time controller design. Instead of constructing recursive Lyapunov functions directly for the original nonlinear system, the proposed method transfers the desired finite-time behavior from a virtual system to the real system through a diffeomorphism. The simulation results from three examples demonstrate the effectiveness of the proposed control laws, showing improved transient performance and better tracking quality compared with the traditional backstepping controller. Future research will aim to extend the proposed approach to high-order nonlinear systems containing model uncertainties and external disturbances.

ACKNOWLEDGEMENTS

This work was supported by a university-level research project at Le Quy Don Technical University under Grant No. 25.01.65.

REFERENCES

Agrachev, A. A., and Sachkov, Y. L. (2005). Geometric control theory (1st ed.). *Moscow: Fizmatlit*.

Amato, F., Ambrosino, R., Ariola, M., Cosentino, C., and De Tommasi, G. (2014). Finite-time stability and control. Lecture Notes in Control and Information Sciences. *Springer London*.

Barbashin, E. A. (1967). Introduction to the theory of stability. *Moscow: Nauka*.

Bhat, S. P., and Bernstein, D. S. (2000). Finite-time stability of continuous autonomous systems. *SIAM Journal on Control and Optimization*, 38(3), 751–766.

Brockett, R. W. (2014). A brief history of the development of geometric nonlinear control. *Automatica*, 50(9), 2203–2220.

Jurdjevic, V. (1997). Geometric control theory. *Cambridge University Press.*

Khalil, H. K. (2003). Nonlinear systems (3rd ed.). *Englewood Cliffs, NJ: Prentice Hall*.

Kim, D. P. (2004). Theory of automatic control: Multidimensional, nonlinear, optimal and adaptive systems (Vol. 2). *Moscow: FIZMATLIT*.

Kolar, B., Schöberl, M., and Diwold, J. (2021). Differential–geometric decomposition of flat nonlinear discrete-time systems. *Automatica,* 132, 109828.

Krasnoshchechenko, V. I., and Krishchenko, A. P. (2005). Nonlinear systems: Geometric methods of analysis and synthesis. Moscow: *Bauman Moscow State Technical University Publishing House*.

Marino, R., and Kokotovic, P. V. (1988). A geometric approach to nonlinear singularly perturbed control systems. *Automatica*, 24(1), 31–41.

Miroshnik, I. V. (2006). Automatic control theory: Nonlinear and optimal systems. *St. Petersburg: Piter*.

Miroshnik, I. V., Nikiforov, V. O., and Fradkov, A. L. (2000). Nonlinear and adaptive control of complex dynamic systems. *St. Petersburg: Nauka*.

Nguyen Xuan, C., Nguyen, H. P., Duc, L. H., Dang, K. T., Kien, L. M., and Pham, T. X. (2019). Building quasi-time-optimal control laws for ball and beam system. In 2019 *3rd International Conference on Recent Advances in Signal Processing, Telecommunications & Computing* (SigTelCom).

Nguyen, X. C., and Pham, X. T. (2025). A finite-time controller design based on strick-feedback system for flexible joint manipulator. *International Journal of Control, Automation, and Systems*, 23(6), 1829–1838.

Pan, Z. (2001). Differential geometric condition for feedback complete linearization of stochastic nonlinear system. *Automatica*, 37(1), 145–149.

Polyakov, A. (2012). Nonlinear feedback design for fixed-time stabilization of linear control systems. *IEEE Transactions on Automatic Control,* 57(8), 2106–2110.

Pupkov, K. A., and Yelutin, N. D. (Eds.). (2004). Methods of modern automatic control theory (2nd ed., Vol. 5). In K. A. Pupkov (Ed.), Methods of classical and modern automatic control theory (784 pages). Moscow: *Publishing House of Bauman Moscow State Technical University*.

Tian, X., Tao, F., Fu, Z., Wang, N., and Song, S. (2023). Fixed-time control based on finite-time observer for Buck converter system with load disturbance. *CEAI,* 25(1), 3–11.

Tong, S. C., Li, Y. M., Feng, G., and Li, T. S. (2011). Observer-based adaptive fuzzy backstepping dynamic surface control for a class of MIMO nonlinear systems. *IEEE Transactions on Systems, Man, and Cybernetics, Part B* (Cybernetics), 41(4), 1124–1137.

Xiao, W., Cao, L., Li, H., and Lu, R. (2020). Observer-based adaptive consensus control for nonlinear multi-agent systems with time-delay. *Science China Information Sciences,* 63(3), 132202.

Yu, J., Shi, P., and Zhao, L. (2018). Finite-time command filtered backstepping control for a class of nonlinear systems. *Automatica*, 92, 173–180.

Zhang, T., Ge, S. S., and Hang, C. C. (2000). Adaptive neural network control for strict-feedback nonlinear systems using backstepping design. *Automatica*, 36(12), 1835–1846.